Am J Transl Res 2021;13(6):5985-6000
www.ajtr.org /ISSN:1943-8141/AJTR0131518

Original Article

PLAC8 gene knockout increases the radio-sensitivity of xenograft tumors in nude mice with nasopharyngeal carcinoma by promoting apoptosis

Li-Jun Shen[1*], Cheng-Lin Qi[1*], Rui Yang[1*], Mao-Ling Huang[1], You Zou[1], Yang Jiang[1], Jian-Fei Sheng[1], Yong-Gang Kong[1], Qing-Quan Hua[1,2], Shi-Ming Chen[1,2]

[1]Department of Otolaryngology-Head and Neck Surgery, Renmin Hospital of Wuhan University, 238 Jie-Fang Road, Wuhan 430060, Hubei, P. R. China; [2]Institute of Otolaryngology-Head and Neck Surgery, Renmin Hospital of Wuhan University, 238 Jie-Fang Road, Wuhan 430060, Hubei, P. R. China. [*]Equal contributors.

Received February 6, 2021; Accepted April 1, 2021; Epub June 15, 2021; Published June 30, 2021

Abstract: In vitro cell experiments showed that knocking out the placenta-specific protein 8 (PLAC8) gene significantly increased the sensitivity of tumor cells to radiation. This study used two nude mouse models of nasopharyngeal carcinoma (NPC) to investigate the radio-sensitization and molecular mechanism of PLAC8 knockout *in vivo*. The expression of PLAC8 in 120 NPC tissues and 30 nasopharyngitis (NPG) tissues was detected by immunohistochemistry (IHC) to analyze the relationship between PLAC8 and neck lymph node metastasis and prognosis in NPC patients. The mRNA expression level of PLAC8 in several NPC cell lines was detected by semi-quantitative RT-PCR. The PLAC8 gene was knocked out in CNE-2 cells using CRISPR/Cas9. The effect of PLAC8 gene knockout on the radiotherapy sensitivity of NPC cells was analyzed by establishing model 1 and model 2 tumor-bearing nude mouse models with two different irradiation methods. The expression of γH2AX, Bax, Bcl-2, Caspase-3 and cleaved Caspase-3 was detected by immunofluorescence (IF), IHC and western blot analysis. PLAC8 expression was significantly increased in NPC tissue samples and NPC cell lines compared with NPG tissue samples and normal cell lines ($P<0.01$). PLAC8 upregulation was associated with lymph node metastasis and a poor prognosis in patients with NPC ($P<0.01$). Both animal models showed that radiotherapy after PLAC8 knockout significantly slowed tumor growth and reduced tumor volume, with tumor inhibition rates of 100% and 66.04%, respectively. In model 2, PLAC8 knockout with radiotherapy increased the expressions of γH2AX, Bax, Caspase-3 and cleaved Caspase-3 but decreased the expression of Bcl-2 ($P<0.01$). In model 1, there was no tumor formation at the site where the cancer cells were injected. The expression levels of γH2AX, Bax, Caspase-3 and cleaved Caspase-3 in skin tissues taken at the injection site were lower than those in NPC tissues treated with radiotherapy, while the expression level of Bcl-2 was higher ($P<0.01$). PLAC8 expression is closely related to neck metastasis and the prognosis of NPC. PLAC8 gene knockout significantly increases the radio-sensitivity of NPC cells *in vivo* by promoting apoptosis, which is an effective strategy for the radiotherapy sensitization of NPC.

Keywords: NPC, PLAC8, radio-sensitivity, apoptosis, subcutaneously transplanted tumor model

Introduction

Nasopharyngeal carcinoma (NPC) is a disease with significant regional and ethnic characteristics that is associated with malignant head and neck tumors. The latest epidemiological statistics showed that by 2018, China had the highest proportion of nasopharyngeal cancer cases in the world, accounting for approximately 47.7%, followed by Indonesia, accounting for 14.2% [1]. Due to the occult location of the disease and the atypical early symptoms, most patients with NPC are already in the middle or late stages when they seek treatment. Based on case statistics of NPC endemic areas, non-keratinizing subtypes account for the majority of cases [2], and this type is usually sensitive to radiation. Therefore, radiotherapy is still the main treatment for NPC. Although NPC is sensitive to radiotherapy, the treatment effectiveness in advanced patients is still unsatisfactory, and the most important reasons are tumor recurrence and distant metastasis caused by radiotherapy resistance [3, 4]. Therefore, it is of

Table 1. PLAC8 expression in NPC and NPG tissues

PLAC8 expression level				
Group	All cases	Upregulation	Downregulation	*p* value
NPC	120	101 (84.2%)	19 (15.8%)	0.000*
NPG	30	14 (46.7%)	16 (53.3%)	

Notes: Samples with a total IRS of 0, 1-3, 4-6 and 7-9 were labeled as (-), (+), (++) and (+++), respectively. Downregulation refers to PLAC8 expression that was labeled as (-) or (+) in clinical tissue samples, while upregulation refers to PLAC8 expression that was labeled as (++) or (+++). *P<0.05.

great importance to improve the radiotherapy sensitivity of patients with NPC.

At present, many studies have explored how to increase the radio-sensitivity of NPC. For example, by regulating target genes such as CKMT1 [5], EMP2 [6] and CPT1A [7] or interfering with miR-24 [8], miR-19b-3p [9] and miR-210 [10], the radio-sensitivity of NPC can be enhanced. In the NPC nude mouse tumor transplantation model established by Tan et al. [7], the tumor volume of the group with downregulated CPT1A combined with radiotherapy was approximately 50% of that of the group received radiotherapy alone, achieving a significant radiotherapy sensitization effect. The study by Kang et al. [8] showed that the tumor inhibition rate was approximately 60% in nude mice bearing xenograft tumor model, confirming that overexpression of miR-24 enhanced the radiotherapy sensitivity of NPC.

Placenta-specific protein 8 (PLAC8) is a small molecule protein that is widely expressed in eukaryotes and plays an important role in normal cellular biological processes and human diseases [11]. There is evidence suggesting that PLAC8 is a key upstream regulator of brown and white adipocyte differentiation [12, 13]. Several studies have shown that PLAC8 is widely involved in the development of various malignancies [14-16]. PLAC8 has been shown to promote epithelial-mesenchymal transformation (EMT) in colon cancer [17]. Lack of PLAC8 inhibits the proliferation of pancreatic cancer cells in vitro and tumor growth *in vivo* [18]. PLAC8 overexpression is associated with a poor prognosis in lung cancer patients [19]. These studies confirm that PLAC8 is a biomarker for new cancer progression.

Our previous studies showed that PLAC8 promotes the invasion and metastasis of NPC cells through the TGF/Smad pathway [20]. In vitro cell experiments showed that PLAC8 gene knockout significantly increased the radio-sensitivity of CNE-2 cells, promoted the apoptosis of CNE-2 cells after radiotherapy, and induced G2/M phase arrest [21]. However, the effect of PLAC8 gene knockout on radio-sensitivity in nude mouse bearing NPC xenograft model is unclear. This study established different radiotherapy animal models of CNE-2 cell xenografts to explore the effect of PLAC8 gene knockout on the radio-sensitivity of NPC cells and related molecular mechanisms, aiming to provide experimental evidence for new radiotherapy sensitization targets for NPC.

Materials and methods

Patient samples and ethical statements

The No. 1501 and No. 1502 tissue arrays were supplied by Guilin Fanpu Biotech (Guangxi, China). PLAC8 expression levels and clinical results were analyzed in samples from 150 patients (120 with NPC and 30 with nasopharyngitis, NPG). All patients provided written informed consent prior to the collection of tissue samples. The general clinical data of these patients are shown in **Table 1**. The tissue chip and animal experimental procedures were approved by the Ethics Review Committee of Wuhan University Renmin Hospital (WDRY-2019-K058) and the Ethics Committee for Animal Experiments of Wuhan University Renmin Hospital (20200815), respectively. Animal testing was conducted in accordance with the National Institutes of Health Guidelines for the Care and Use of Laboratory Animals. All efforts were made to minimize the suffering of laboratory animals.

Cell lines, cell culture conditions and irradiation methods

The human NPC cell line CNE-2 was purchased from the Chinese Typical Culture Preservation Center of Wuhan University. Other cell lines (the human NPC cell lines HK1, SUNE1, 5-8F, and 6-10B and the amorphic nasopharyngeal epithelial cell line NP69) were purchased from the Laboratory of Molecular Tumor Pathology (Southern Medical University). PLAC8-knockout CNE-2 cells, hereafter referred to as koPLAC8 CNE-2 cells, were established by Beijing Bio-

cytogen Company (Beijing, China, http://www.bbctg.com.cn/index/index/index.html) by using CRISPR/Cas9 technology [22]. CNE-2 and koPLAC8 CNE-2 cells were cultured in RPMI-1640 medium (Biosun) containing 10% fetal bovine serum (Gibco). NP69 cells were cultured in serum-free medium for keratinocytes (KSFM) (Invitrogen) supplemented with bovine epidermal growth factor (EGF) (BD Biosciences). All cells were cultured in an incubator at 37°C with 5% CO_2 and 95% saturated humidity [23].

For cell irradiation, after cells were seeded in culture plates and allowed to adhere overnight, the cells were transferred to a medical linear accelerator (Radiology Center, Renmin Hospital of Wuhan University, Varian Accelerator, 23ex) for irradiation. A single dose of 8 Gy at 600 cGy/min was used for room temperature vertical irradiation for 1 min, with an SSD=100 cm [21].

For animal irradiation, the animals were transferred to a medical linear accelerator (Radiology Center, Renmin Hospital of Wuhan University, Varian Accelerator, 23ex) for fixation and then irradiated after inhalation anesthesia with isoflurane (induction concentration of 4% and maintenance concentration of 1-2%). A single dose of 8 Gy at 600 cGy/min was used for room temperature vertical irradiation for 1 min using a lead plate to cover the tumor-free portion of the body during irradiation. The tumor was covered with a compensation membrane with a thickness of approximately 1 cm. The irradiation method was single local irradiation with an SSD=100 cm, as previously described [8].

RNA extraction and semi-quantitative RT-PCR

Total RNA was extracted using TRIzol reagent (Life Technologies, Carlsbad, USA) and converted to cDNA using a reverse transcription kit (Thermo Scientific, Rockford, USA). A SYBR Green PCR kit (Roche, Germany) was used for semi-quantitative reverse transcription polymerase chain reaction (RT-PCR). GAPDH was used as the internal control. The relative quantitative value (RQ) was used as the basis for quantitative comparisons of target gene expression between the two groups. The RT-PCR primers for PLAC8 (5'-GGAACAAGCGTCGCAATGAG-3'; 5'-AAAGTACGCATGGCTCTCCTT-3') and GAPDH (5'-GAGAAGGCTGGGGCTCATTT-3'; 5'-TAAGCAGTTGGTGGTGCAGG-3') were purchased from Hundred Thousand Degree Biotechnology Co., Ltd. The $2^{-\Delta\Delta CT}$ method was used to analyze the mRNA expression level [24].

Establishment of subcutaneous xenotransplant tumor model 1 (model 1)

Male BALB/c-nu mice (n=12; 4-6 weeks of age, 15-20 g) were obtained from Vital River Laboratory Animal Technology (Beijing, China) and housed in the SPF barrier facility of the Animal Experiment Center of Wuhan University Renmin Hospital. The nude mice were randomly divided into two groups: group A: IR+CNE-2; and group B: IR+koPLAC8 CNE-2 (both n=6). CNE-2 and koPLAC8 CNE-2 cells in logarithmic growth phase were exposed to 8 Gy and cultured for 24 h (1×10^6; IR+CNE-2 or IR+koPLAC8 CNE-2) and then subcutaneously injected into the back of each mouse to establish a subcutaneous xenograft model of NPC. After 3 weeks, all the mice were sacrificed. Tumor tissue was collected for further analysis. The long and short diameters of the tumors were measured every 3 days. Tumor volume was calculated as follows: long diameter × short diameter^2/2 [19]. If there was no transplanted tumor growth in the nude mice, the skin tissue corresponding to the injection site of the NPC cells was collected for subsequent detection. There were 6 samples in each group of tumors or skin tissues, 3 of which were fixed with fixation fluid for paraffin embedding, and the other 3 were stored at -80°C for western blot analysis. The tumor growth inhibition rate was calculated as follows: (%) = $(V_{\text{Control group}} - V_{\text{Experimental group}})/V_{\text{Control group}} \times 100\%$ [25].

Establishment of subcutaneous xenotransplant tumor model 2 (model 2)

Male BALB/c-nu mice (n=12; 4-6 weeks of age, 15-20 g) were randomly divided into two groups: group A: IR+CNE-2; and group B: IR+koPLAC8 CNE-2 (both n=6). The cells (1×10^6; IR+CNE-2 or IR+koPLAC8 CNE-2) were subcutaneously injected into the back of each mouse, and the long and short diameters of the tumors were measured every day. On the sixth day after the inoculation, the tumors of the nude mice were exposed to a single dose of 8 Gy once for 1 min. When the average tumor volume of a group of mice reached 1500 mm^3, the mice were sacrificed, and the tumor tissues were collected for further detection and analysis [24]. There were 6 samples in each group of

tumors or skin tissues, 3 of which were fixed with fixation fluid for paraffin embedding, and the other 3 were stored at -80°C for western blot analysis. The tumor growth inhibition rate was calculated as follows: (%) = ($V_{Control\ group}$ - $V_{Experimental\ group}$)/$V_{Control\ group}$ ×100% [25].

Hematoxylin and eosin (HE) staining and immunofluorescence (IF)

The tumor tissues and skin tissues were soaked in 4% paraformaldehyde and fixed for 2 days. After dehydration with low to high concentrations of alcohol, the tissues were placed in xylene, cleared and embedded in paraffin. The sections were sliced at a thickness of 5 μm and stained with HE. Paraffin-embedded sections were dewaxed with xylene, rehydrated with gradient alcohol, and blocked with 5% bovine serum albumin in PBS (Beyotime, Shanghai, China) for 30 min. The sections were then incubated overnight with target protein-specific antibodies at 4°C, such as γH2AX, Bax, Bcl-2, Caspase-3 and cleaved Caspase-3 (CST, Boston, USA).

The sections were then incubated with a PE-conjugated secondary antibody (CST, Boston, USA) at 37°C for 2 h. IF staining was used to observe the expression of target proteins in the tissue samples of transplanted mouse tumors. All images were taken using a fluorescence microscope (Olympus BX-51, Japan) [20]. IF analysis was performed as described previously [26].

Immunohistochemistry (IHC) analysis

IHC was used to detect the expression levels of target proteins in patient samples and nude mouse tumor samples. Paraffin-embedded tissue sections were dewaxed and rehydrated in xylene and gradient alcohol solution, and antigen repair was performed with citrate solution for 5 min. After antigen repair and blocking, the primary antibody was incubated overnight at 4°C. The secondary antibody was then incubated at room temperature for 1 h. Finally, diaminobenzidine (DAB) was used to visualize the staining. Image-Pro Plus 6.0 (Media Cybernetics, MD, USA) was used to analyze the results. The primary antibodies were as follows: Bax, Bcl-2, Caspase-3 and cleaved Caspase-3 (CST, Boston, USA). Staining was scored according to previously described standards [19].

The cumulative optical density (IOD) of several fields was calculated by using ImageJ software, and the average optical density (AOD) (cumulative optical density IOD/total field) was calculated. The experiment was repeated three times to calculate the average.

Western blot analysis

Western blotting was used to detect the expression levels of target proteins in nude mouse tumor samples. Total protein was collected after lysing the cells with RIPA buffer containing protease inhibitors (Beyotime, Shanghai, China). After quantifying the concentration of total protein, an equal amount of total protein (40 μg) was separated by 10% sodium dodecyl sulfate-polyacrylamide gel electrophoresis (SDS-PAGE; Beyotime, Shanghai, China). Next, target proteins were transferred to polyvinylidene fluoride membranes and blocked for 1 h with 5% nonfat milk. Membranes were incubated separately overnight at 4°C with the following primary antibodies: PLAC8 (1:1000), Bcl-2 (1:1000), Bax (1:1000), γH2AX (1:1000) and GAPDH (1:2000) (Cell Signaling Technology, Danvers, USA). Then, the membranes were incubated with IRDye 680RD-conjugated secondary antibodies (Licor, NE, USA) at room temperature for 1 h. Each membrane was scanned and quantified using the Odyssey infrared imaging system (Licor, NE, USA). GAPDH was used as the reference protein.

Statistical analysis

All experiments were repeated three times. SPSS software version 22.0 (SPSS, Chicago, USA) was used for statistical analysis. Enumeration data are presented as the mean ± standard error of the mean (SEM), and differences between two groups were tested by the t-test. Data of clinical tumor samples were statistically analyzed using the χ^2 test. The survival curve was determined by the log-rank Kaplan-Meier method. A value of $P<0.05$ was considered statistically significant.

Results

Expression of the PLAC8 protein in NPC tissues and PLAC8 mRNA in NPC cell lines

First, we analyzed PLAC8 expression in human NPC tissue chips and NPC cell lines.

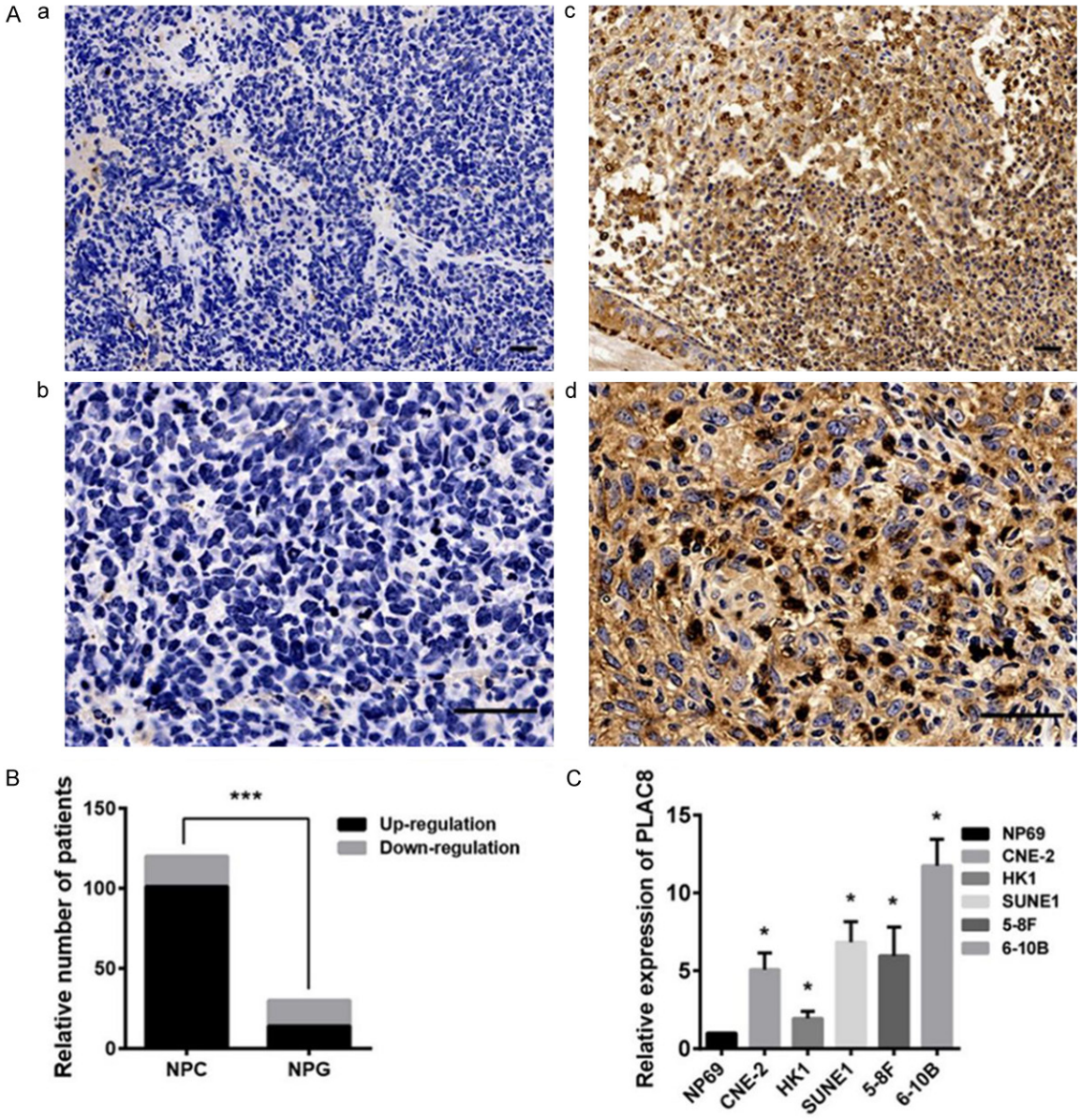

Figure 1. Expression of the PLAC8 protein in NPC tissues and PLAC8 mRNA in NPC cell lines. (A) IHC results of tissue samples from patients with NPG and NPC. (a/b and c/d) indicate NPG negative expression and NPC strong positive expression, respectively. Image magnification in (a/c and b/d): ×100 and ×400, respectively. (B) PLAC8 expression in NPC tissues was higher than that in NPG tissues (n=150, ***P<0.001). (C) RT-PCR showed higher PLAC8 mRNA levels in human NPC cell lines (CNE-2, HK1, SUNE1, 5-8F, and 6-10B) than in NP69 cell lines. Data are shown as the mean ± standard error of the mean of three technical replicates (*P<0.05).

PLAC8 protein expression rate in NPC specimens (84.2%, 101/120) was significantly higher than that in NPG specimens (46.7%, 14/30) (P<0.01, **Table 1**; **Figure 1A**, **1B**). Next, we measured PLAC8 mRNA expression in nasopharyngeal epithelial cells (NP69) and human NPC cells and found that PLAC8 mRNA expression was higher in human NPC cells than in NP69 cells (**Figure 1C**).

The relationship between PLAC8 expression in NPC tissues and clinical parameters of NPC patients

Further analysis of the relationship between PLAC8 expression in NPC samples and neck lymph node metastasis and survival time showed that NPC patients with PLAC8 upregulation were more likely to have neck lymph node

Table 2. PLAC8 expression in NPC samples and its associations with patient clinicopathological data

PLAC8 expression level				
Item	All cases	Upregulation	Downregulation	*p* value
Sex				0.645
Male	90	62 (68.9%)	28 (31.1%)	
Female	30	22 (73.3%)	8 (26.7%)	
Age (years)				0.867
≥.8	42	29 (69.0%)	13 (31.0%)	
<50	78	55 (70.5%)	23 (29.5%)	
Neck mass				0.000*
Yes	76	62 (81.6%)	14 (18.4%)	
No	44	10 (22.7%)	34 (77.3%)	

Notes: Samples with a total IRS of 0, 1-3, 4-6 and 7-9 were labeled as (-), (+), (++) and (+++), respectively. Downregulation refers to PLAC8 expression that was labeled as (-) or (+) in clinical tissue samples, while upregulation refers to PLAC8 expression that was labeled as (++) or (+++). *P<0.05.

metastasis than those with PLAC8 downregulation (**Table 2**; **Figure 2A-C**). The survival curve suggested that patients with PLAC8 downregulation had a better prognosis than those with PLAC8 upregulation (**Figure 2D**). These results confirmed that PLAC8 was significantly overexpressed in NPC tissues and human NPC cells and was associated with neck lymph node metastasis and a low survival rate. It was found that gender did not affect the PLAC8 expression level (P>0.05, **Table 2**).

PLAC8 knockout significantly increased the radio-sensitivity of NPC cells in vivo

In this study, we analyzed changes in the radiosensitivity of PLAC8-knockout NPC cells *in vivo* by establishing two xenograft tumor models in nude mice. In model 1, CNE-2 cells and koPLAC8 CNE-2 cells were externally irradiated and directly injected subcutaneously into nude mice. In model 2, CNE-2 cells and koPLAC8 CNE-2 cells were injected subcutaneously into nude mice to form tumors, and then the tumors were irradiated.

In model 1, subcutaneous grafts of IR+CNE-2 cells grew gradually and reached their maximum on day 21. However, subcutaneous grafts of IR+koPLAC8 CNE-2 cells grew gradually up to 9 days after injection, but the growth was slow. After that, the tumors gradually shrank, completely disappeared on day 12, and did not reappear by day 21. The tumor volume was recorded as "0". To analyze the structure of the injection site, we harvested skin tissue at the site where the CNE-2 cells were injected for subsequent analysis (**Figure 3A**). In model 2, the tumor volume of the IR+CNE-2 and IR+koPLAC8 CNE-2 groups increased gradually before radiotherapy, but the tumor growth of the IR+koPLAC8 CNE-2 group was significantly slower than that of the IR+CNE-2 group. When the nude mice were sacrificed 15 days after inoculation, the average tumor volumes of the transplanted tumors in the two groups were 1.571±0.055 cm^3 and 0.533±0.132 cm^3. The tumor inhibition rate in the IR+koPLAC8 CNE-2 group was 66.04% (**Figure 3A**).

The tumor tissues in the IR+CNE-2 group in model 1 and the two groups in model 2 were collected. The tumor surface appeared smooth to the naked eye (**Figure 3A**). After HE staining, the tumor tissue was observed under an optical microscope and showed a solid structure with large tumor cells, large and deeply stained nuclei, prominent nucleoli, and visible mitotic images (**Figure 3B**). However, no tumor cells were observed following HE staining in the nude mouse skin tissue from the IR+koPLAC8 CNE-2 group in model 1 (**Figure 3B**).

IF revealed the differential expression of γH2AX, Bax, Bcl-2, Caspase-3 and cleaved Caspase-3 in tumors

To understand the possible mechanism by which PLAC8 knockout increases radio-sensitivity, IF staining was used to visually observe the differential expression of γH2AX, Bax, Bcl-2, Caspase-3 and cleaved Caspase-3 in each group. In model 1, the fluorescence intensity of γH2AX, Bax, Caspase-3 and cleaved Caspase-3 in the skin tissues of the IR+koPLAC8 CNE-2 group was significantly lower than that of the tumor tissues of the IR+CNE-2 group, while the fluorescence intensity of Bcl-2 was significantly higher than that of the IR+CNE-2 group (**Figure 4A**, **4C**), confirming that the apoptosis of normal skin tissues was significantly less than that of NPC tissues after receiving radiotherapy. In model 2, the fluorescence intensity of γH2AX, Bax, Caspase-3 and cleaved Caspase-3 in the IR+koPLAC8 CNE-2 group was

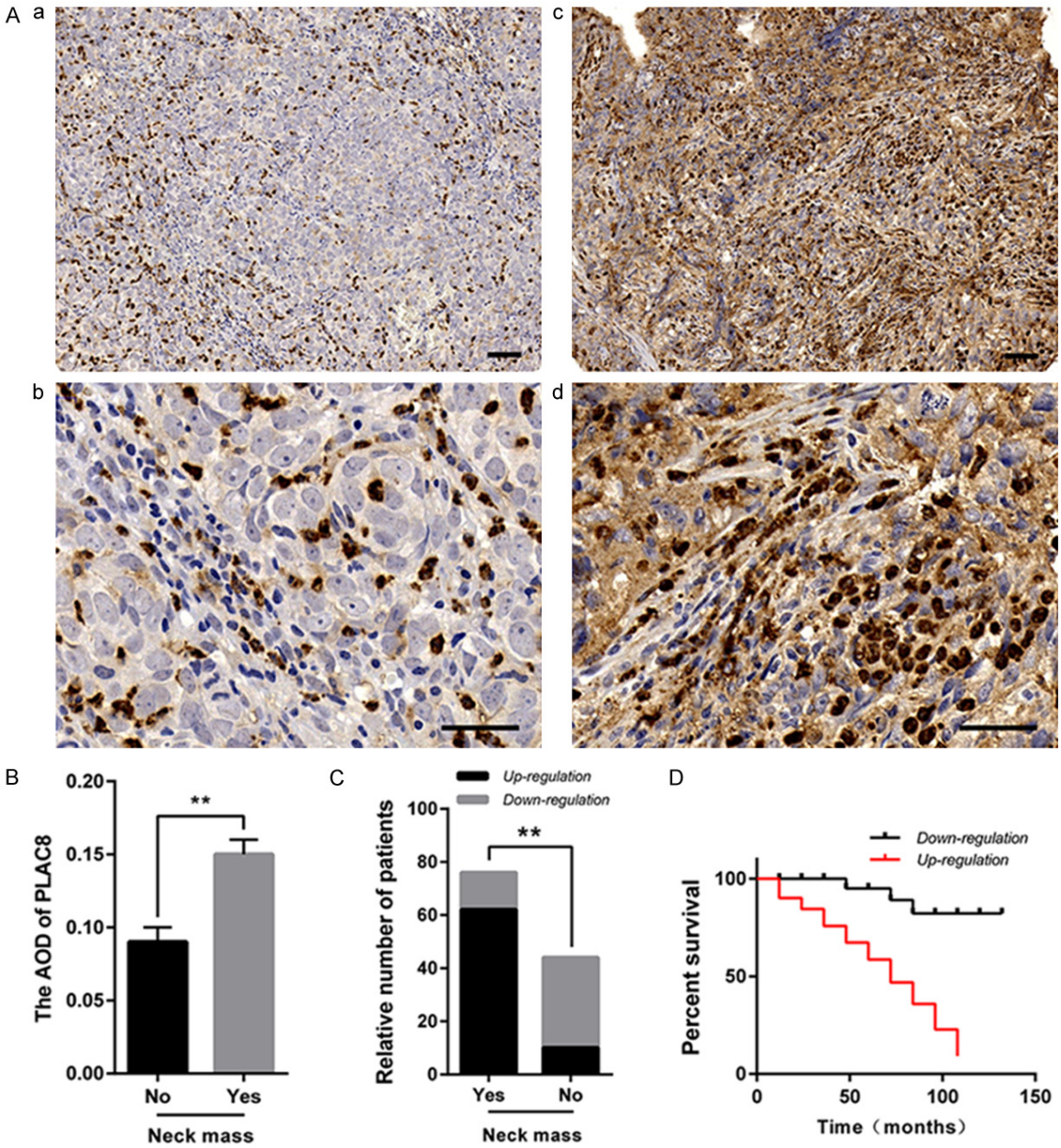

Figure 2. Expression of PLAC8 in NPC tissues and its relationship with clinical characteristics. (A) IHC results of tissue samples from NPC patients without neck lymph node metastasis. (a and b) are the IHC results of tissues without neck lymph node metastasis, while (c and d) are the IHC results of tissues with neck lymph node metastasis. Image magnification in (a/c and b/d): ×100 and ×400, respectively. (B) Quantitative analysis of PLAC8 in NPC tissues. (C) PLAC8 was upregulated in the majority of NPC patients with neck metastasis (n=120, **P<0.01). (D) Survival curves suggest that patients with NPC and low PLAC8 expression have a prolonged survival time (n=120, P<0.01).

higher than that in the IR+CNE-2 group, while the fluorescence intensity of Bcl-2 was lower than that in the IR+CNE-2 group (**Figure 4B**, **4D**), confirming that cancer cell apoptosis increased after radiotherapy *in vivo* with PLAC8 knockout.

IHC detection of the differential expression of γH2AX, Bax, Bcl-2, Caspase-3 and cleaved Caspase-3 in tumors

After IHC staining, brown-yellow particles were observed under an optical microscope, indicat-

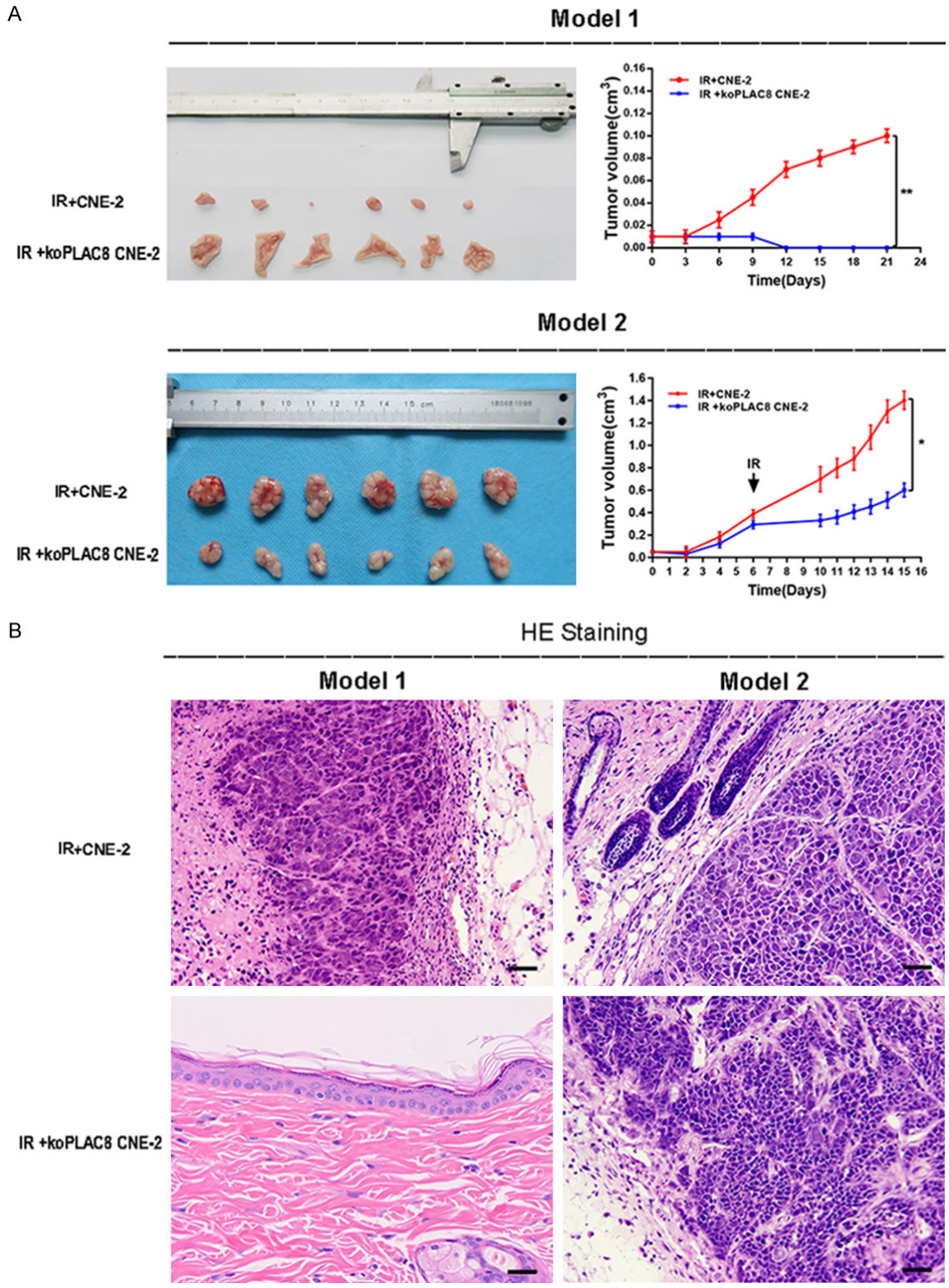

Figure 3. Both models confirmed that knockout of the PLAC8 gene increased the radio-sensitivity of NPC cells. After exposure to both irradiation methods, complete tumors were obtained from the IR+CNE-2 and IR+koPLAC8 CNE-2 tumor-bearing nude mouse models. A. In model 1, the tumors of nude mice in the IR+koPLAC8 group disappeared, and the tissue at the inoculation site (shown) was collected. In model 1 and model 2, there was a significant difference in tumor volume after irradiation (n=6, *P<0.05, **P<0.01). B. In model 1, the tissue at the inoculation site was confirmed as skin tissue by HE staining. Image magnification: ×200.

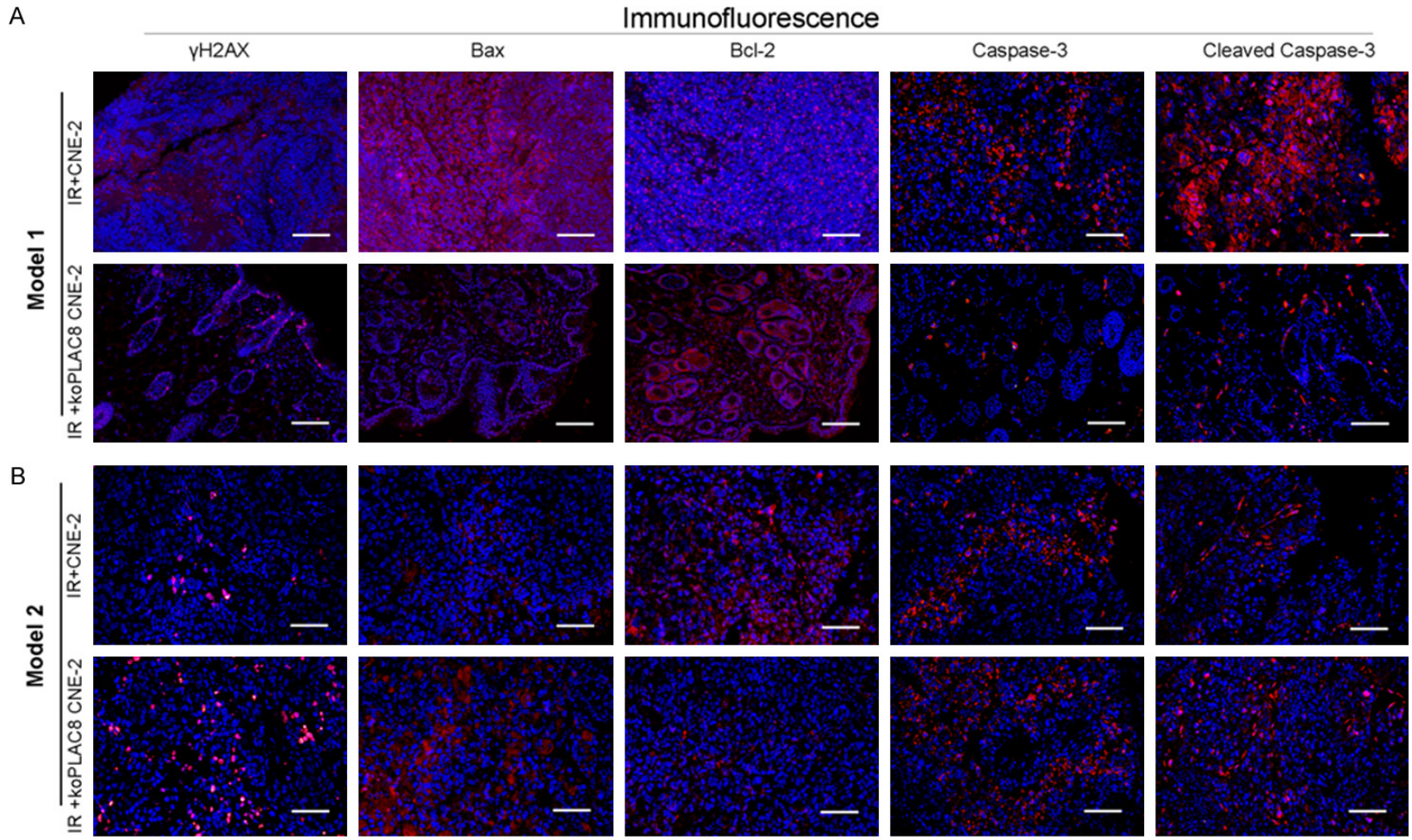
A
Immunofluorescence
γH2AX
Bax
Bcl-2
Caspase-3
Cleaved Caspase-3
Model 1
IR+CNE-2
IR +koPLAC8 CNE-2
B
Model 2
IR+CNE-2
IR +koPLAC8 CNE-2

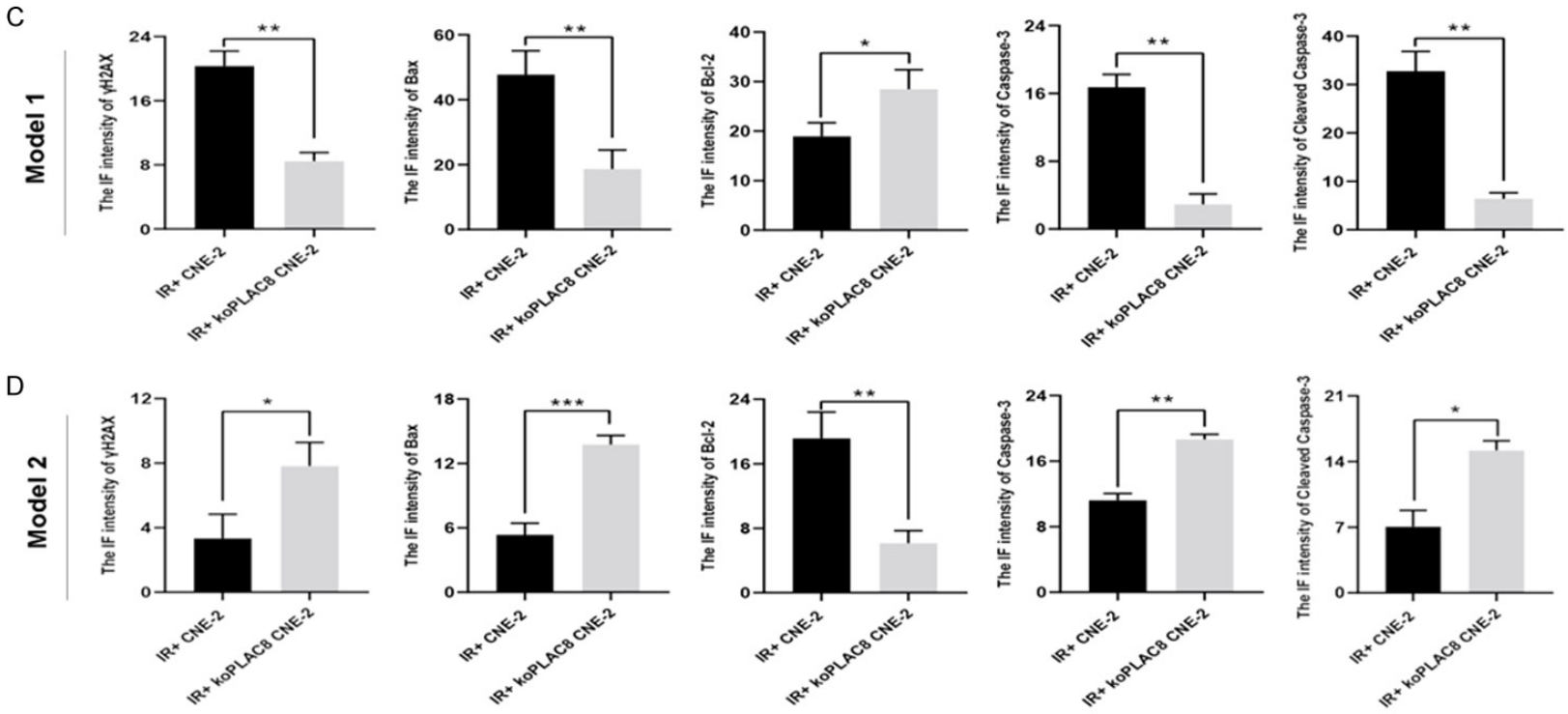

Figure 4. Expression of γH2AX, Bax, Bcl-2, Caspase-3 and cleaved Caspase-3. A. Protein staining with IF in the IR+CNE-2 and IR+koPLAC8 CNE-2 groups in model 1. B. Protein staining with IF in the IR+CNE-2 and IR+koPLAC8 CNE-2 groups in model 2. C. In model 1, compared with the fluorescence intensity in the tumor tissues of the IR+CNE-2 group, the skin tissues of the IR+koPLAC8 CNE-2 group had weaker fluorescence of γH2AX, Bax, Caspase-3 and cleaved Caspase-3, while that of Bcl-2 was stronger. D. In model 2, compared with the fluorescence intensities in the IR+CNE-2 group, those of γH2AX, Bax, Caspase-3 and cleaved Caspase-3 in the IR+koPLAC8 CNE-2 group were stronger, while that of Bcl-2 was weaker (red fluorescence indicates positive expression, while blue fluorescence indicates DAPI staining). Image magnification: ×200. *P<0.05, **P<0.01, ***P<0.001.

ing positive expression. The results showed that in model 1, the AODs of γH2AX, Bax, Caspase-3 and cleaved Caspase-3 in the IR+koPLAC8 CNE-2 group were significantly lower than those in the IR+CNE-2 group (**Figure 5A**, **5C**), while the AOD of Bcl-2 was significantly higher than that in the control group (P<0.05), confirming that apoptosis in normal skin tissue was significantly less than that in NPC cells receiving radiotherapy. In model 2, the AODs of γH2AX, Bax, Caspase-3 and cleaved Caspase-3 in the IR+koPLAC8 CNE-2 group were significantly higher than those in the IR+CNE-2 group (**Figure 5B**, **5D**), while the AOD of Bcl-2 was the opposite (P<0.01), confirming that apoptosis was increased in PLAC8-knockout cancer cells after radiotherapy *in vivo*.

Western blot detection of the differences in PLAC8, γH2AX, Bax and Bcl-2 in tumor tissues

In model 1, the expression levels of PLAC8, γH2AX and Bax in the skin tissues of the IR+koPLAC8 CNE-2 group were significantly lower than those of the IR+CNE-2 group (P<0.05), while the expression of Bcl-2 was significantly higher (**Figure 6A**). This confirmed that there was significantly less apoptosis in normal skin tissues than in NPC tissues treated with radiotherapy. In model 2, the IR+koPLAC8 CNE-2 group showed almost no expression of PLAC8 (compared with the IR+CNE-2 group) (**Figure 6B**), confirming that PLAC8 was successfully knocked out. In this group, the protein expressions of γH2AX and Bax were significantly increased (**Figure 6B**), while the protein expression of antiapoptotic protein Bcl-2 was significantly decreased (P<0.05), confirming that PLAC8 knockout promoted the apoptosis of NPC cells *in vivo* after radiotherapy.

Discussion

High expression of PLAC8 is associated with the development of many cancers [8, 18, 27]. To investigate whether PLAC8 is associated with the clinical biology of NPC, we performed histological analysis. The results showed that the expression level of PLAC8 in NPC tissues was significantly higher than that in NPG tissues, and the upregulation of PLAC8 was closely related to neck metastasis and a poor prognosis in NPC patients. Subsequently, we found that PLAC8 mRNA expression was significantly higher in a variety of NPC cell lines than in immortalized nasopharyngeal epithelial cell lines. These results confirm that PLAC8 is one of the oncogenes associated with nasopharyngeal cancer. Nasopharyngeal carcinoma incidence is higher in males than in females, with a ratio of about 2.5 in China [1]. According to our data presented in **Table 2**, gender did not affect the PLAC8 expression level. In the following study, only male mice were selected as model animals to ensure homogeneity of the experiment on the one hand and to simulate the gender characteristics of most patients with nasopharyngeal carcinoma on the other hand.

CRISPR/Cas9 technology is one of the most effective methods used to knock out specific genes [28]. In our previous studies, we successfully knocked out the PLAC8 gene in CNE-2 cell lines using this technique [20, 21]. The advantage of this knockout method is that the knockout is efficient and can be passed to the next generation. In model 2, there was almost no expression of the PLAC8 protein in tumor tissue in the PLAC8-knockout group, confirming that the PLAC8 gene was indeed knocked out in CNE-2 cells.

In this study, two different subcutaneous xenotransplant tumor models of 1 and 2 were established. In Model 1, PLAC8-knockout CNE-2 cells were treated with radiotherapy in vitro and then inoculated in nude mice. In Model 2, PLAC8-knockout CNE-2 cells were inoculated in nude mice and then treated with radiotherapy. Our aim was to compare the difference in efficacy between these two tumor models and the possible causes.

There was an increasing separation trend in the tumor growth curves of model 1 and model 2, and the number of transplanted tumors with PLAC8 gene knockout was significantly smaller than that without. In model 2, the tumor inhibition rate of PLAC8 gene knockout was as high as 66.04% after 10 days of radiotherapy, while in model 1 (with PLAC8 gene knockout), no significant tumor tissue growth was observed between 13 and 23 days after radiotherapy, confirming that PLAC8 gene knockout combined with radiotherapy significantly inhibited the growth and proliferation of NPC cells *in vivo*.

In model 1, we found that the knockout of PLAC8 followed by radiotherapy in nude mice resulted in relatively slow tumor growth in the

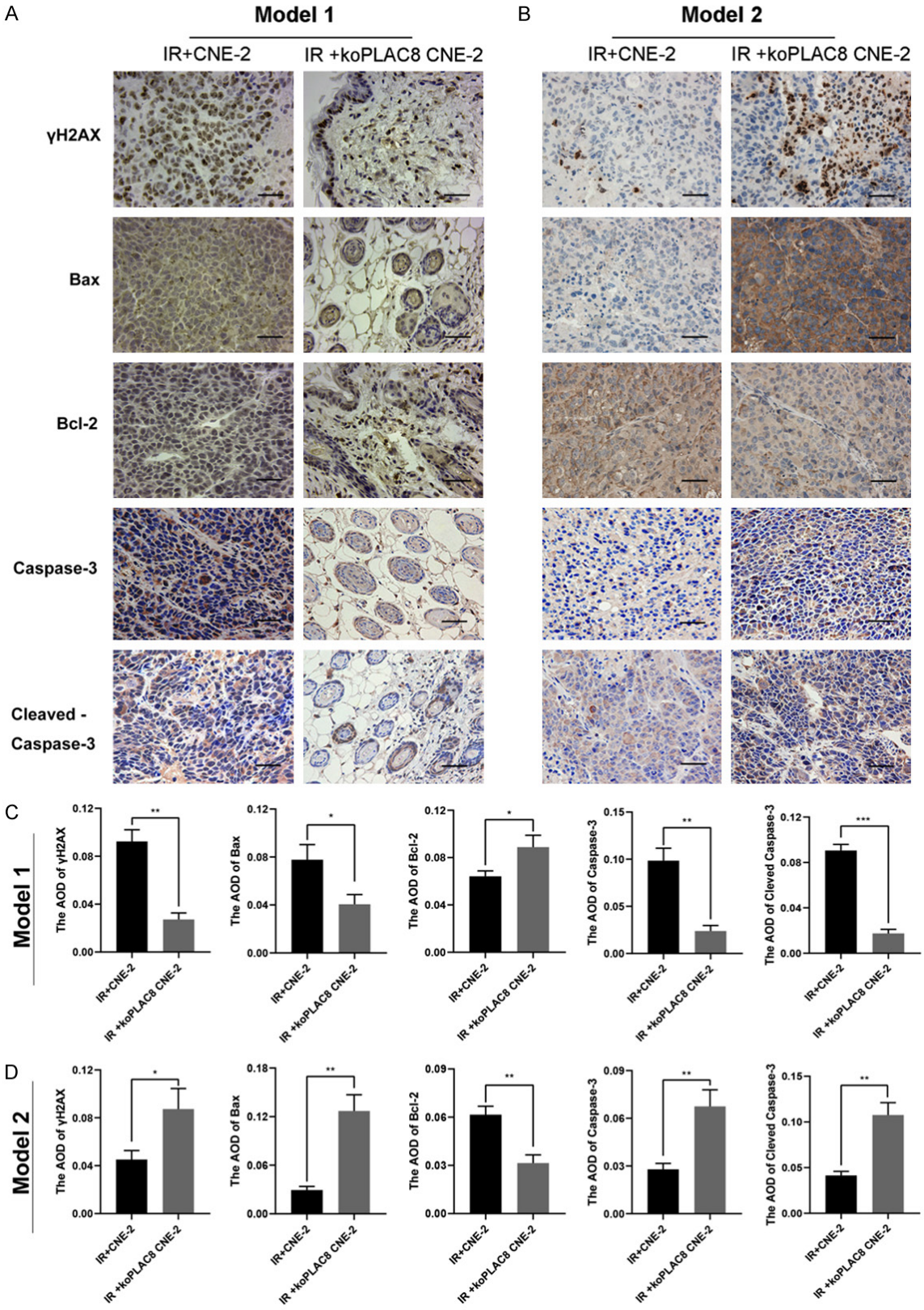

Figure 5. Staining and quantitative analysis of γH2AX, Bax, Bcl-2, Caspase-3 and cleaved Caspase-3 expression under an optical microscope. A. Protein staining in the IR+CNE-2 and IR+koPLAC8 CNE-2 groups in model 1. B. Protein staining in the IR+CNE-2 and IR+koPLAC8 CNE-2 groups in model 2. C. The expression of γH2AX, Bax, Caspase-3 and cleaved Caspase-3 was significantly lower in the IR+koPLAC8 CNE-2 group than that in the IR+CNE-2 group,

while that of Bcl-2 was significantly higher. D. The expression of γH2AX, Bax, Caspase-3 and cleaved Caspase-3 was significantly higher in the IR+koPLAC8 CNE-2 group than that in the IR+CNE-2 group, while that of Bcl-2 was lower (brown-yellow particles indicate positive staining, while blue indicates nuclear staining). Image magnification: ×200. *P<0.05, **P<0.01, ***P<0.001.

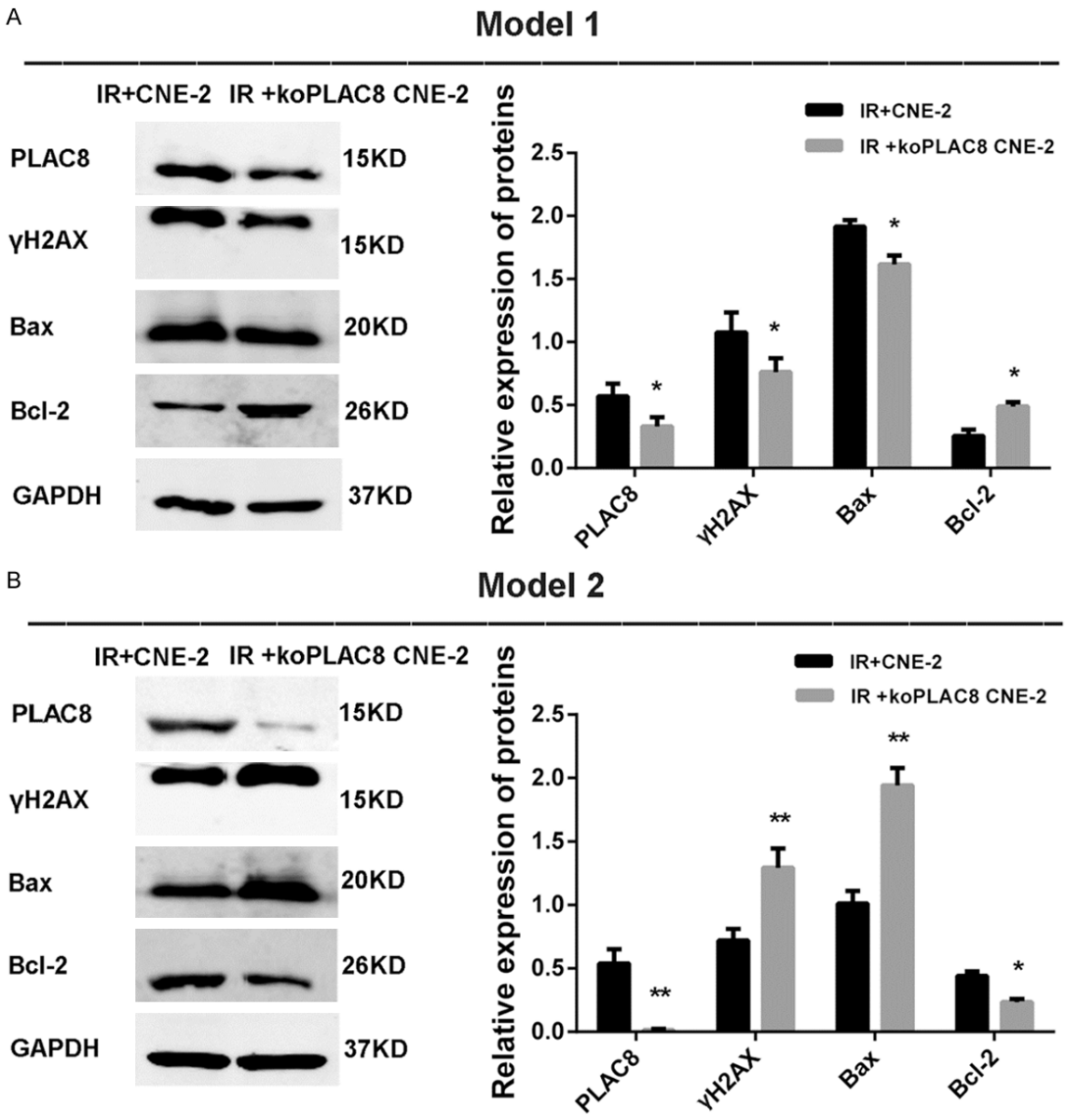

Figure 6. Knockout of PLAC8 enhanced radio-sensitivity by activating the apoptotic pathway. A. Target protein bands obtained by western blot analysis and their statistical graph in model 1. B. Target protein bands obtained by western blot analysis and their statistical graph in model 2. Data are shown as the mean ± standard error of the mean of three technical replicates (*P<0.05, **P<0.01).

first 9 days. However, the tumor completely disappeared by day 12, and no tumor growth was observed by day 24. The tumor inhibition rate in model 1 was higher than that in model 2. The reason may be that all CNE-2 cells in model 1 were exposed to radiation, while some tumor cells in model 2 were not exposed to radiation. In addition, in model 2, the growth rate of the PLAC8-knockout group was slightly slower than that of the control group before receiving radiotherapy, demonstrating that PLAC8 knockout alone partially inhibited tumor growth, consis-

tent with our previous experimental results [20].

DNA double-strand rupture is a very important type of cell damage caused by radiation. During DNA damage repair, the histone phosphorylation of H2AX (γH2AX) occurs rapidly in a double-strand break reaction [29]. IHC, IF and western blotting experiments in model 2 confirmed that γH2AX protein expression in the tissue of CNE-2-transplanted tumors with PLAC8 knockout was significantly higher than that without. The animal model with CNE-2-transplanted tumors exposed to radiation had increased DNA double-strand breakage, and DNA repair CNE-2-transplanted tumor tissue was more sensitive to radiation after PLAC8 knockout.

During tumor growth, in addition to the abnormal proliferation of cancer cells, the apoptosis of cancer cells is blocked. This study further analyzed the effect of PLAC8 gene knockout on the apoptosis of CNE-2 cells *in vivo* by analyzing tumor tissue apoptosis. Bax and Bcl-2 are the most important pro- and antiapoptotic proteins in the Bcl-2 family, respectively, and play an important regulatory role in the apoptotic signaling pathway in tumor cells [30]. Model 2 demonstrated that PLAC8 gene knockout and radiation treatment significantly increased the expression of the proapoptotic protein Bax and decreased the expression of the apoptotic suppressor protein Bcl-2, which may be one of the molecular mechanisms by which PLAC8 gene knockout increases the radio-sensitivity of CNE-2 cell grafts.

The cysteine protease (Caspase) family plays a key role in cell apoptosis and is one of the most important apoptotic markers, among which Caspase-3 is considered to be the main executor and an important effector of cell apoptosis [31]. Cleaved Caspase-3 is the activated form of Caspase-3. In model 2, the results showed that the protein expression levels of Caspase-3 and cleaved Caspase-3 in the tumor tissue of the PLAC8-knockout group were significantly higher than those of the control group. Combined with the above experimental results of Bax and Bcl-2, we hypothesized that the main mechanism by which PLAC8 gene knockout improves the radiotherapy sensitivity of NPC may be the activation of apoptotic signaling pathway.

Since the nude mice in the radiotherapy plus PLAC8 knockout group in model 1 were sacrificed without tumors at the original subcutaneous implantation site, the skin tissues at the implantation site were retained for subsequent experimental analysis. The results showed that the expression levels of γH2AX, Bax, Caspase-3 and cleaved Caspase-3 in skin tissues were lower than those in NPC tumor tissues, while the expression level of Bcl-2 was higher, consistent with the different expression levels of these pro- and antiapoptotic proteins in normal and tumor tissues after radiotherapy. In model 1, PLAC8 was expressed in skin tissue, but its expression was higher in NPC tumor tissue, which also confirmed that PLAC8 is an oncogene.

According to the results of this study, PLAC8 knockout can exert the effect of radiotherapy sensitization by inducing apoptosis. Our previous study confirmed that PLAC8 contributes to radio-resistance in NPC by inhibiting the PI3K/AKT/GSK3β pathway [21]. Furthermore, Mao et al. confirmed that PLAC8 contributes to cell proliferation and suppresses cell apoptosis in breast cancer by activating the PI3K/AKT/NF-κB pathway [15]. Therefore, similar to the increased radiotherapy sensitivity of cultured cells, the molecular mechanism of the increased radiotherapy sensitivity of NPC cells *in vivo* may be related to the PLAC8-regulated AKT signaling pathway.

In summary, this study demonstrated that PLAC8 gene knockout significantly increased the radio-sensitivity of xenograft NPC tumors in nude mice by promoting apoptosis. PLAC8 is an effective target for the radiotherapy sensitization of NPC.

Acknowledgements

This work was supported by the National Natural Science Foundation of China [grant number: 81770981] and by the Hubei Province Health and Family Planning Scientific Research Project [grant numbers: WJ2019M186 and WJ2019M195]. We would like to acknowledge the staff of the Laboratory Animal Center of Renmin Hospital of Wuhan University for their help in breeding the animals.

Disclosure of conflict of interest

None.

Address correspondence to: Shi-Ming Chen and Qing-Quan Hua, Department of Otolaryngology-Head and Neck Surgery, Renmin Hospital of Wuhan University, 238 Jie-Fang Road, Wuhan 430060, Hubei, P. R. China. E-mail: shimingchen0468@163.com (SMC); hqqrm@sina.com (QQH)

References

[1] Chen YP, Chan ATC, Le QT, Blanchard P, Sun Y and Ma J. Nasopharyngeal carcinoma. Lancet 2019; 394: 64-80.

[2] Carioli G, Negri E, Kawakita D, Garavello W, La Vecchia C and Malvezzi M. Global trends in nasopharyngeal cancer mortality since 1970 and predictions for 2020: focus on low-risk areas. Int J Cancer 2017; 140: 2256-2264.

[3] Tian Y, Yan M, Zheng J, Li R, Lin J, Xu A, Liang Y, Zheng R and Yuan Y. miR-483-5p decreases the radiosensitivity of nasopharyngeal carcinoma cells by targeting DAPK1. Lab Invest 2019; 99: 602-611.

[4] Wang C, Su Z, Hou H, Li D, Pan Z, Tian W and Mo C. Inhibition of anaphase-promoting complex by silence APC/C(Cdh1) to enhance radiosensitivity of nasopharyngeal carcinoma cells. J Cell Biochem 2017; 118: 3150-3157.

[5] Lan R, Huang F, Zhong G, Chen R, Wang Z, Chen J, Fu L, Hong J and Zhang L. Effects of CKMT1 on radiosensitivity of nasopharyngeal carcinoma cells. Int J Radiat Biol 2019; 95: 597-606.

[6] Tang M, Liu RY, Zhou C, Yuan MZ, Wu DM, Yuan Z, Zhang P and Lang JY. EMP2 re-expression inhibits growth and enhances radiosensitivity in nasopharyngeal carcinoma. Tumour Biol 2017; 39: 1010428317695972.

[7] Tan Z, Xiao L, Tang M, Bai F, Li J, Li L, Shi F, Li N, Li Y, Du Q, Lu J, Weng X, Yi W, Zhang H, Fan J, Zhou J, Gao Q, Onuchic JN, Bode AM, Luo X and Cao Y. Targeting CPT1A-mediated fatty acid oxidation sensitizes nasopharyngeal carcinoma to radiation therapy. Theranostics 2018; 8: 2329-2347.

[8] Kang M, Xiao J, Wang J, Zhou P, Wei T, Zhao T and Wang R. MiR-24 enhances radiosensitivity in nasopharyngeal carcinoma by targeting SP1. Cancer Med 2016; 5: 1163-1173.

[9] Huang T, Yin L, Wu J, Gu JJ, Wu JZ, Chen D, Yu HL, Ding K, Zhang N, Du MY, Qian LX, Lu ZW and He X. MicroRNA-19b-3p regulates nasopharyngeal carcinoma radiosensitivity by targeting TNFAIP3/NF-kappaB axis. J Exp Clin Cancer Res 2016; 35: 188.

[10] Li BY, Luo Y, Zhao WS, Zhang L, Zhou HJ, Zou YC and Zhang T. MicroRNA210 negatively regulates the radiosensitivity of nasopharyngeal carcinoma cells. Mol Med Rep 2017; 16: 1401-1408.

[11] Song WY, Hortensteiner S, Tomioka R, Lee Y and Martinoia E. Common functions or only phylogenetically related? The large family of PLAC8 motif-containing/PCR genes. Mol Cells 2011; 31: 1-7.

[12] Jimenez-Preitner M, Berney X and Thorens B. Plac8 is required for white adipocyte differentiation in vitro and cell number control in vivo. PLoS One 2012; 7: e48767.

[13] Jimenez-Preitner M, Berney X, Uldry M, Vitali A, Cinti S, Ledford JG and Thorens B. Plac8 is an inducer of C/EBPbeta required for brown fat differentiation, thermoregulation, and control of body weight. Cell Metab 2011; 14: 658-670.

[14] Sun Y, Lai X, Yu Y, Li J, Cao L, Lin W, Huang C, Liao J, Chen W, Li C, Yang C, Ying M, Chen Q and Ye Y. Inhibitor of DNA binding 1 (Id1) mediates stemness of colorectal cancer cells through the Id1-c-Myc-PLAC8 axis via the Wnt/beta-catenin and Shh signaling pathways. Cancer Manag Res 2019; 11: 6855-6869.

[15] Mao M, Chen Y, Jia Y, Yang J, Wei Q, Li Z, Chen L, Chen C and Wang L. PLCA8 suppresses breast cancer apoptosis by activating the PI3k/AKT/NF-kappaB pathway. J Cell Mol Med 2019; 23: 6930-6941.

[16] Gong K, Gong ZJ, Lu PX, Ni XL, Shen S, Liu H, Wang JW, Zhang DX, Liu HB and Suo T. PLAC8 overexpression correlates with PD-L1 upregulation and acquired resistance to chemotherapies in gallbladder carcinoma. Biochem Biophys Res Commun 2019; 516: 983-990.

[17] Li C, Ma H, Wang Y, Cao Z, Graves-Deal R, Powell AE, Starchenko A, Ayers GD, Washington MK, Kamath V, Desai K, Gerdes MJ, Solnica-Krezel L and Coffey RJ. Excess PLAC8 promotes an unconventional ERK2-dependent EMT in colon cancer. J Clin Invest 2014; 124: 2172-2187.

[18] Kaistha BP, Lorenz H, Schmidt H, Sipos B, Pawlak M, Gierke B, Kreider R, Lankat-Buttgereit B, Sauer M, Fiedler L, Krattenmacher A, Geisel B, Kraus JM, Frese KK, Kelkenberg S, Giese NA, Kestler HA, Gress TM and Buchholz M. PLAC8 localizes to the inner plasma membrane of pancreatic cancer cells and regulates cell growth and disease progression through critical cell-cycle regulatory pathways. Cancer Res 2016; 76: 96-107.

[19] Jia Y, Ying X, Zhou J, Chen Y, Luo X, Xie S, Wang QC, Hu W and Wang L. The novel KLF4/PLAC8 signaling pathway regulates lung cancer growth. Cell Death Dis 2018; 9: 603.

[20] Huang ML, Zou Y, Yang R, Jiang Y, Sheng JF, Han JB, Kong YG, Tao ZZ and Chen SM. Placenta specific 8 gene induces epithelial-mesenchymal transition of nasopharyngeal carcinoma cells via the TGF-beta/Smad pathway. Exp Cell Res 2019; 374: 172-180.

[21] Yang R, Tao ZZ, Huang ML, Zheng YF, Dai MY, Zou Y and Chen SM. Knockout of the placenta specific 8 gene radiosensitizes nasopharyngeal carcinoma cells by activating the PI3K/AKT/GSK3beta pathway. Am J Transl Res 2018; 10: 455-464.

[22] Tang XR, Wen X, He QM, Li YQ, Ren XY, Yang XJ, Zhang J, Wang YQ, Ma J and Liu N. MicroRNA-101 inhibits invasion and angiogenesis through targeting ITGA3 and its systemic delivery inhibits lung metastasis in nasopharyngeal carcinoma. Cell Death Dis 2017; 8: e2566.

[23] Xie P, Yu H, Wang F, Yan F and He X. Inhibition of LOXL2 enhances the radiosensitivity of castration-resistant prostate cancer cells associated with the reversal of the EMT process. Biomed Res Int 2019; 2019: 4012590.

[24] Sun D, Mu Y and Piao H. MicroRNA-153-3p enhances cell radiosensitivity by targeting BCL2 in human glioma. Biol Res 2018; 51: 56.

[25] Park YG, Choi J, Jung HK, Kim B, Kim C, Park SY and Seol JW. Baicalein inhibits tumor progression by inhibiting tumor cell growth and tumor angiogenesis. Oncol Rep 2017; 38: 3011-3018.

[26] Kasten BB, Jiang K, Cole D, Jani A, Udayakumar N, Gillespie GY, Lu G, Dai T, Rosenthal EL, Markert JM, Rao J and Warram JM. Targeting MMP-14 for dual PET and fluorescence imaging of glioma in preclinical models. Eur J Nucl Med Mol Imaging 2020; 47: 1412-1426.

[27] Kolluru V, Pal D, Papu John AMS, Ankem MK, Freedman JH and Damodaran C. Induction of Plac8 promotes pro-survival function of autophagy in cadmium-induced prostate carcinogenesis. Cancer Lett 2017; 408: 121-129.

[28] Demirci Y, Zhang B and Unver T. CRISPR/Cas9: an RNA-guided highly precise synthetic tool for plant genome editing. J Cell Physiol 2018; 233: 1844-1859.

[29] Kunogi H, Sakanishi T, Sueyoshi N and Sasai K. Prediction of radiosensitivity using phosphorylation of histone H2AX and apoptosis in human tumor cell lines. Int J Radiat Biol 2014; 90: 587-593.

[30] Mirakhor Samani S, Ezazi Bojnordi T, Zarghampour M, Merat S and Fouladi DF. Expression of p53, Bcl-2 and Bax in endometrial carcinoma, endometrial hyperplasia and normal endometrium: a histopathological study. J Obstet Gynaecol 2018; 38: 999-1004.

[31] Xu B, Mao Z, Ji X, Yao M, Chen M, Zhang X, Hang B, Liu Y, Tang W, Tang Q and Xia Y. miR-98 and its host gene Huwe1 target Caspase-3 in Silica nanoparticles-treated male germ cells. Sci Rep 2015; 5: 12938.